

# Deep Eutectic Solvent Choline Chloride/*p*-toluenesulfonic Acid and Water Favor the Enthalpy-Driven Binding of Arylamines to Maleimide in Aza-Michael Addition

Abelardo Gutiérrez-Hernández, Arlette Richaud, Luis Chacón-García, Carlos J. Cortés-García, Francisco Méndez,\* and Claudia Araceli Contreras-Celedón\*

Cite This: <https://dx.doi.org/10.1021/acs.joc.0c02039>

Read Online

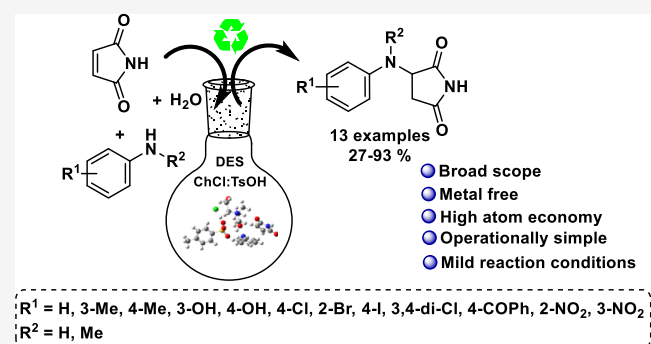
ACCESS |

Metrics & More

Article Recommendations

Supporting Information

**ABSTRACT:** Deep eutectic solvents (DESs) have been considered “the organic reaction medium of the century” because they can be used as solvents and active catalysts in chemical reactions. However, experimental and theoretical studies are still needed to provide information on the structures of DESs, the kinetics and thermodynamics properties, the interactions between the DESs and the substrates, the effect of water on the DES supramolecular network and its physicochemical properties, and so forth. This information is very useful to understand the essence of the processes that take place in the catalysis of chemical reactions and, therefore, to help in the design of a DES for a specific reaction and sample. This article shows a systematic study of the impact of DES choline chloride/*p*-toluenesulfonic acid and DES choline chloride/*p*-toluenesulfonic acid–water in the aza-Michael addition of arylamines to maleimide to obtain aminopyrrolidine-2,5-dione derivatives. The derivatives are obtained under very mild reaction conditions with good yield. The global reaction is exothermic, spontaneous, permitted by enthalpy, and prohibited for entropy. The calculated potential energy surface shows a reaction mechanism of six steps controlled by enthalpy (except the last step that is controlled by entropy). The water incorporated in the supramolecular DES complex stabilizes the transition states and favors the enthalpy-driven binding. A set of H/D exchange NMR experiments validates the transition state existing in the fourth stage of the mechanism.



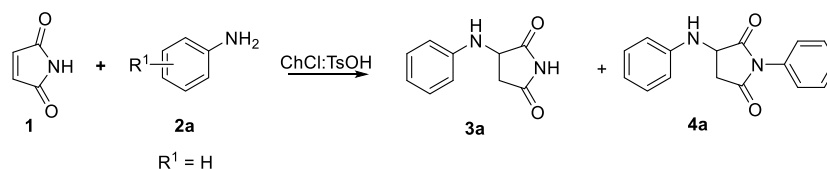
## 1. INTRODUCTION

One of the great challenges concerning the chemical industry in the 21st century is the replacement of conventional toxic solvents by sustainable solvents obtained from renewable sources, thus trying to minimize industrial waste to promote a sustainable environment.<sup>1</sup> A large part of the development in chemistry takes place or is carried out in liquid solution; therefore, the correct choice of the solvent used in a chemical reaction is of crucial importance<sup>2–5</sup> because in addition to the chemical and physical characteristics of the solvent itself, several aspects must be taken into account from an ecological point of view, such as its nature, boiling point, flammability, toxicity, and biodegradability, among others.<sup>6,7</sup> Thus, the so-called neoteric solvents have emerged as important options, such as fluorinated solvents, supercritical fluids, ionic liquids, and deep eutectic solvents (DESs), all of which have a number of advantages and disadvantages.<sup>8–11</sup> DESs are generated with the highest atomic economy from a mixture of two or more immiscible solid components (Brønsted or Lewis acids and bases) under a phase change to liquid at a precise temperature; their formation is simple,<sup>12,13</sup> they do not generate byproducts, and no purification is required before use.<sup>14–18</sup> The toxicity of

DESs is very low or null and DESs<sup>19,20</sup> possess high biodegradability and<sup>21</sup> negligible vapor pressures, are recyclable and reusable, and easily allow the solubility of organic and inorganic compounds as a result of their high polarity. In addition to the possibility of modifying their viscosity and density properties varying the composition,<sup>22</sup> for example, adding a third component such as carboxylic acid, halide, or water<sup>23–29</sup> makes DESs very versatile and taken into account as the ideal solvent for various purposes.<sup>30–34</sup> Several papers have been published in this area,<sup>35–38</sup> and the authors have concluded that systematic studies of the DESs are necessary to better understand their physicochemical properties and provide information on the definition, nature, and structure of DES,<sup>39,40</sup> the kinetic, thermodynamic, and dynamic of the

Received: August 23, 2020

Table 1. Reaction Condition of Aza-Michael Addition to Maleimide 1



entry	1/2a <sup>a</sup>	reaction condition <sup>b</sup>	3a yield <sup>c</sup> (%)	4a yield <sup>c</sup>
1	1:1	120 °C, 1 h	9	n. o. <sup>g</sup>
2	1:2	120 °C, 0.5 h	35	traces
3	1:3	120 °C, 1.5 h	12	7%
4	1:5	120 °C, 20 h	19	17%
5	1:2	120 °C, 22 h	44	40%
6	1:2	90 °C, 2 h	82	traces
7	1:2	50 °C <sup>d</sup> , 1.5 h	93	n. o. <sup>g</sup>
8	1:2	RT <sup>e</sup> , 20 h	65	n. o. <sup>g</sup>
9	1:2	RT <sup>f</sup> , 20 h	42	n. o. <sup>g</sup>

<sup>a</sup>Maleimide 1, aniline 2a ratio. <sup>b</sup>0.097 g (1 equiv) maleimide 1, 0.186 g (2 equiv) aniline 2a, 0.5 g DES ChCl/TsOH 1:1. <sup>c</sup>Product yield. <sup>d</sup>0.3 mL of H<sub>2</sub>O was added. <sup>e</sup>1 mL of H<sub>2</sub>O was added. <sup>f</sup>1 mL of H<sub>2</sub>O was used as a solvent. <sup>g</sup>Not observed by <sup>1</sup>H NMR.

interactions with the substrates,<sup>41–44</sup> and, specially, the effect of water on DESs' supramolecular network. This information is very valuable and useful to understand the essence of the processes that take place in the catalysis of chemical reactions and, therefore, to help in the design of a DES for a specific reaction and reagents.

In this article, we make for the first time a systematic study of the impact of DES choline chloride/*p*-toluenesulfonic acid ChCl/TsOH and DES choline chloride/*p*-toluenesulfonic acid–water ChCl/TsOH/H<sub>2</sub>O in the aza-Michael addition of arylamines 2 to maleimide 1 to obtain aminopyrrolidine-2,5-dione derivatives 3 under very mild reaction conditions with high yield. The derivatives are of great importance in biology, materials science, and chemistry; they are used as synthetic blocks to obtain small bioactive molecules, natural products, drugs, and agrochemicals.<sup>45–53</sup> This contribution complements our previous work on nucleophilic addition reactions in  $\alpha,\beta$ -unsaturated carbonyl compounds (maleimide and maleic anhydride)<sup>54–56</sup> that were made in terms of the local hard and soft acid and base principle and the density functional theory.<sup>57–60</sup> Now, our experimental and theoretical studies on the aza-Michael addition have been motivated for two overarching goals: (i) development of a new experimental methodology under mild reaction conditions for fast and efficient synthesis of 3, through the aza-Michael additions of 2 to 1 using ChCl/TsOH and water as solvents without the need of a catalyst, ligand, and/or additive and (ii) understanding the kinetics and thermodynamics of the interactions between ChCl/TsOH and the reagents and the effect of water on the supramolecular network of ChCl/TsOH using spectroscopic techniques and a potential energy surface.

The aza-Michael conjugate addition<sup>61,62</sup> is recognized as a simple synthetic strategy for facilitating the addition of compounds with nucleophilic nitrogen to compounds  $\alpha,\beta$ -unsaturated and to encourage the formation of N–C bonds generally with good yields. This reaction has been widely studied with different nucleophilic nitrogen and different acceptors of Michael; however, very few have been performed with maleimides.<sup>63–65</sup> The conjugate addition of primary or secondary amines to maleimides proceeds with good results when long reaction times, high temperatures, and high pressures are used. Under these reaction conditions,

maleimides have serious reactivity problems because they present a high tendency to polymerization as well as a greater facility to be hydrolyzed under basic conditions, which makes them difficult to obtain good results in the formation of  $\beta$ -aminocarbonyl derivatives, thus limiting their usefulness and application. In recent years, some methods have been described to obtain selectivity in the addition of amines to maleimides. Harris and Philp described the use of bis-(phosphine oxide) as a reagent with polarization effect to accelerate the nucleophilic addition of amines to maleimides.<sup>66</sup> Papamicaël described that the presence of TMEDA or *trans*-TMCDA accelerating the speed of the reaction promotes chemoselectivity to the addition.<sup>67</sup> Workentin used AuNPs as a template macromolecule to modify maleimides under hyperbaric pressure conditions (11,000 atm).<sup>68</sup> Scheidt described the conjugate addition of alkylamines to maleimides, with Ca<sup>2+</sup> complexes<sup>69</sup> and under cooperative catalysis with a Lewis acid and a Brønsted base.<sup>70</sup> However, it is very important to describe new methods that can be used as synthetic tools to obtain aminopyrrolidine-2,5-dione and that avoid the need of using drastic conditions and the use of metal catalysts, that improve the performance of the expected products, and that avoid the formation of undesirable products.

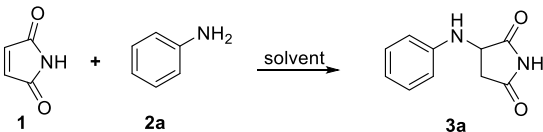
## 2. RESULTS AND DISCUSSION

We commenced our investigation with the reaction of maleimide 1 and aniline 2a in the presence of ChCl/TsOH (1:1) as a solvent (Table 1) under an open atmosphere. First, 1 equiv maleimide 1 and 1 equiv aniline 2a in ChCl/TsOH were allowed to react at 120 °C for 1 h, generating the expected product 3a in 9% yield (entry 1). Encouraged by this result, various ratios of raw materials were screened, and 3a was obtained in several yields (entries 2–4), suggesting that 1 equiv maleimide 1 and 2 equiv aniline 2a was the best ratio. However, increasing the time reaction to 22 h did not improve the yield of 3a (entry 5) but favored the synthesis of 4a in 40% yield. When the temperature was decreased to 90 °C for 2 h, 3a was produced in 82% yield (entry 6). To carry out the reaction at lower temperatures, we added water to the reaction medium; we observed that when we added 0.3 mL of water, the reaction was carried out at 50 °C, and after 1.5 h, we obtained 3a in 93% yield (entry 7). Considering that the

addition of water favored the best agitation of the reaction mixture and increased the **3a** yield, in the following essay, we decided to add 1 mL of water and carry out the reaction at room temperature; under these conditions, the formation of **3a** was observed in 65% yield after 20 h (entry 8). In another test, we used only water as a solvent and observed 42% of **3a** (entry 9).

Next, when the model reaction was screened in different DES, **3a** was produced in 64, 61, and 87% (Table 2). In

**Table 2. Reaction Condition of Aza-Michael Addition to Maleimide 1**



entry	solvent	reaction condition <sup>a</sup>	<b>3a</b> yield
1	ChCl/urea 1:2	50 °C, 1.5 h	64% <sup>c</sup>
2	ChCl/ZnCl <sub>2</sub> 1:2	50 °C, 1.5 h	61% <sup>c</sup>
3	ChCl/tartaric Ac. 1:2	70 °C, 1.5 h	87%
4	MeOH <sup>b</sup>	60 °C, 20 h	21%
5	THF <sup>b</sup>	60 °C, 20 h	18%
6	toluene <sup>b</sup>	60 °C, 20 h	11%
7	cyclohexane <sup>b</sup>	60 °C, 20 h	n. o. <sup>d</sup>

<sup>a</sup>0.097 g (1 equiv) maleimide **1**, 0.186 g (2 equiv) aniline **2a**, 0.5 g DES. <sup>b</sup>1 mL of organic solvent. <sup>c</sup>**3a** was observed in traces by <sup>1</sup>H NMR. <sup>d</sup>Not observed by <sup>1</sup>H NMR.

different polar or nonpolar solvents such as methanol, THF, and toluene, **3a** was produced in 21, 18, and 11% yields, respectively. No formation of compound **3a** was observed in cyclohexane under the reaction conditions used.

With the optimized conditions in hand, the scope of the reaction was explored by reacting maleimide **1** with different aromatic amines **2b–2m**. The reaction of **2b** or **2c** bearing electron-donating groups as CH<sub>3</sub> on the aromatic ring with **1** generated the products **3b** and **3c** in 80 and 85% yields, respectively, while that of **2d** and **2e** afforded **3d** and **3e** in 42 and 27% yields, respectively. On the other hand, the treatment of **1** with electron-withdrawing groups as 4-chloro, 2-bromo, 4-iodo, and 3,4-dichloro, on the amine aromatic ring produced **3f**, **3g**, **3h**, and **3i**, gave 84, 43, 91, and 40% yields, respectively. When **2j**, **2k**, and **2l** were used, **3j**, **3k**, and **3l** were produced in 80, 57, and 37% yields, respectively. When we used **2m**, a secondary aromatic amine, the desired product **3m**, was obtained with a 90% yield (Figure 1). Ruesgas-Ramón et al. (2017) pointed out that “the extraction process is affected by several factors: affinity between DESs and the target compounds, the water content, the mole ratio between DES’ starting molecules, the liquid/solid ratio between the DES and sample, and the conditions and extraction method”.<sup>71</sup> Fortunately, for our case, the extractions of DES were high because in most of the reactions, the addition products were the only ones that were formed. We will return to this point in the theoretical section.

As we can observe from Table 1, the reaction of maleimide **1** with aniline **2a** to obtain 3-(phenylamino)pyrrolidine-2,5-dione **3a** is favored with the presence of ChCl/TsOH and water. Therefore, we decided to explore the potential energy surface to obtain the kinetic and thermodynamic properties of the reaction and identify the structures, degree of participation,

and interactions of ChCl/TsOH and water with the substrate. To study the principles governing the stability of the species, we have constructed the model using directly the molecules of the reagents **1** and **2a** and the solvents ChCl, TsOH, and water. The ground-state geometries and energies of **1**, **2a**, **3a**, ChCl, TsOH, H<sub>2</sub>O, complex **C**, intermediate **I**, transition states **TSs**, and product **P** (see Scheme 1) were obtained at the M062X/6-311++G(d,p) level of theory<sup>72</sup> using GAUSSIAN09.<sup>73</sup> M062X is a well-balanced functional that includes dispersion corrections and properly describes the interaction energies for charge-transfer complexes.<sup>74,75</sup> Frequency calculations confirmed that the local minimum and transition states have 0 and 1 imaginary frequencies, respectively. Scheme 1 shows the aza-Michael reaction mechanism of five steps for the addition of **2a** to **1** and six steps for the addition in the presence of ChCl, TsOH, and H<sub>2</sub>O.

Figure 2 shows the energy profiles for the addition (the relative electronic energies including zero-point energy corrections); the red line shows the addition in the absence of molecules of the solvent and water (**P** is **3a**), and the blue and green lines show the addition in the presence of ChCl/TsOH and ChCl/TsOH/H<sub>2</sub>O, respectively. The energy profiles are almost similar, but they differ mainly in that the reactions in the presence of ChCl/TsOH and ChCl/TsOH/H<sub>2</sub>O occur in the low and deepest energy curves, respectively, and all the species are more stable than the reagents, including the transition states.

**2.1. First Step: 1 + 2a → C.** As the reagents **1** and **2a** approach to form **C**, the energy decreases −7.0 kcal/mol (red line in Figure 2), −51.9 kcal/mol (with ChCl/TsOH, blue line), and −63.0 kcal/mol (with ChCl/TsOH/H<sub>2</sub>O, green line). The great stability of **C** with ChCl/TsOH/H<sub>2</sub>O occurs by the interactions between the oxygen atom of the O=C group of maleimide and the hydrogen atoms of the −CH<sub>3</sub> group of ChCl, and the −NH<sub>2</sub> group of aniline with the H<sub>2</sub>O and the sulfonic moiety of TsOH (see Scheme 2). It is interesting to know that Chandrasekhar and Jorgensen (1985) have found a (Cl⋯CH<sub>3</sub>C)<sup>−</sup> complex in the nucleophilic substitution reaction of Cl<sup>−</sup> + CH<sub>3</sub>C.<sup>76</sup>

**2.2. Second Step: C → [TS1]<sup>‡</sup>.** Then, **C** overcomes an activation barrier for the addition of 34.6, 21.6 kcal/mol (with ChCl/TsOH), and 20.2 kcal/mol (with ChCl/TsOH/H<sub>2</sub>O) and forms the intermediate **I** via the first transition state **TS1** (Scheme 3). Strictly speaking, the activation energy for the addition (the difference of energy between **TS1** and the separate reagents) is just 27.6 kcal/mol. However, there is no activation barrier between separate reagents and **TS1** in the presence of ChCl/TsOH and ChCl/TsOH/H<sub>2</sub>O; the activation energy has a negative value of −30.3 and −42.8 kcal/mol, respectively (see Figure 2).

**2.3. Third and Fourth Steps: [TS1]<sup>‡</sup> → I → [TS2]<sup>‡</sup>.** The new N–C bond obtained in the intermediate **I** makes a tetravalent nitrogen atom and a trivalent carbon atom in the aniline and maleimide moieties, respectively (see Scheme 4). Then, the energy increases to get the second transition state **TS2**; the activation energies are 11.4, 14.3 kcal/mol (with ChCl/TsOH), and 2.6 kcal/mol (with ChCl/TsOH/H<sub>2</sub>O).

Scheme 5 shows **TS2** that involves the deprotonation and protonation of the nitrogen and carbon atoms of the aniline and maleimide moieties, respectively. The proton transfer process involves a 1,3-hydrogen shift rearrangement, and it occurs internally (H–N–C–C → N–C–C–H) with the formation of a four-membered ring; in general, the process

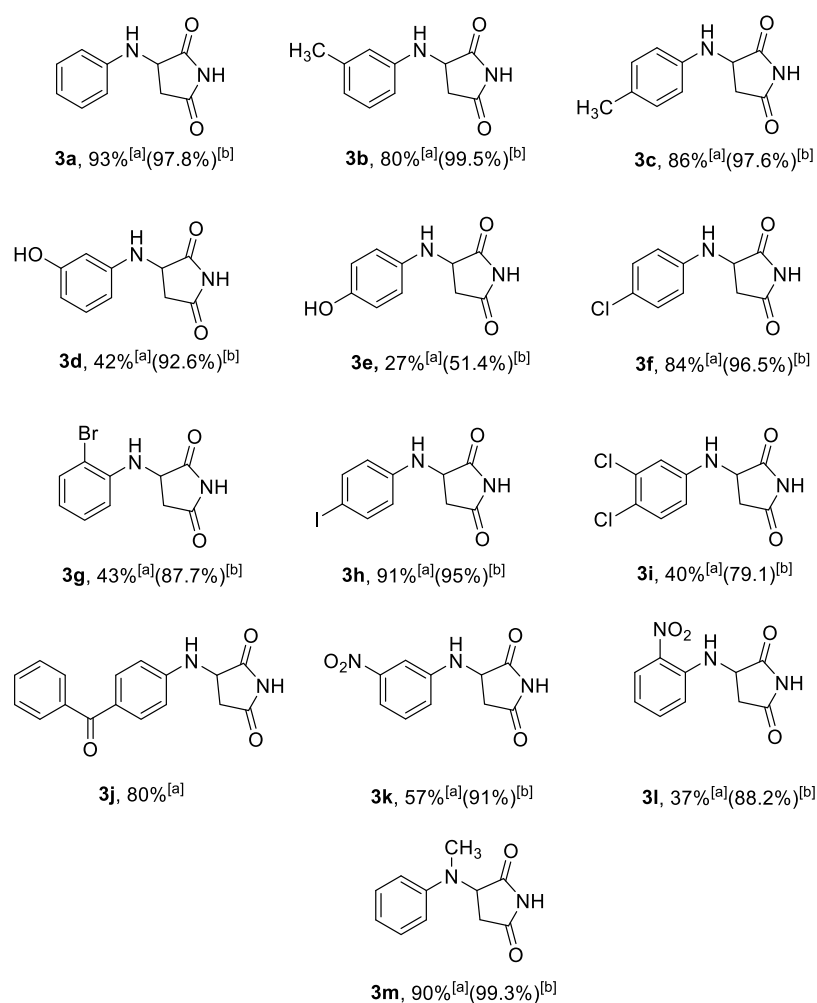
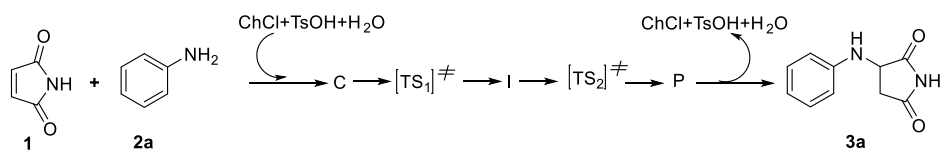


**Figure 1.** Synthesized aminopyrrolidine-2,5-dione **3a–3m**. (a) Isolated yield (b) conversions were calculated by GC analysis of the limiting substrate and final product.

### Scheme 1. Reaction Mechanism of Aza-Michael Addition to Maleimide **1**



occurs with high energy, and we can observe that **TS2** is less stable than the reagents (maleimide and aniline) by 36.6 kcal/mol. For **TS2** with  $\text{ChCl}/\text{TsOH}$ , the four-membered ring is stabilized by 16.1 kcal/mol. In the case of **TS2** with  $\text{ChCl}/\text{TsOH}/\text{H}_2\text{O}$ , the process involves a six-membered ring where the water molecule accepts a proton from the N atom and donates a proton to the C atom; **TS2** is stabilized by 41.9 kcal/mol.

**2.4. Fifth Step:  $[\text{TS2}]^\ddagger \rightarrow \text{P}$ .** As we can observe in **Figure 2**, the more stable species is **P**; its energy decreases with respect to the reagents to  $-20.7$ ,  $-61.0$  kcal/mol (with  $\text{ChCl}/\text{TsOH}$ ), and  $-73.8$  kcal/mol (with  $\text{ChCl}/\text{TsOH}/\text{H}_2\text{O}$ ) (see **Scheme 6**).

**Table 3** displays the relative electronic energies  $\Delta E$ , enthalpies  $\Delta H^\circ$ , Gibbs free energies  $\Delta G^\circ$ , and  $T\Delta S^\circ$  (in kcal/mol) for all the species involved in the additions: (i) **1** + **2a**, (ii) **1** + **2a** +  $\text{ChCl}/\text{TsOH}$ , and (iii) **1** + **2a** +  $\text{ChCl}/\text{TsOH}/\text{H}_2\text{O}$ . The thermochemical properties were calculated at the M062X/6-311++G(d,p) level of theory<sup>72</sup> using

GAUSSIAN09.<sup>73</sup> They were obtained at  $T = 298.15$  K, and  $P = 1$  atm by means of partition functions using statistical thermodynamic relationships.<sup>73</sup> The global reactions (i) **1** + **2a**  $\rightarrow$  **P** ( $\Delta G^\circ = -8.3$  kcal/mol and  $\Delta H^\circ = -21.2$  kcal/mol), (ii) **1** + **2a** +  $\text{ChCl}/\text{TsOH} \rightarrow \text{P}$  ( $\Delta G^\circ = -23.7$  kcal/mol and  $\Delta H^\circ = -60.4$  kcal/mol), and (iii) **1** + **2a** +  $\text{ChCl}/\text{TsOH}/\text{H}_2\text{O} \rightarrow \text{P}$  ( $\Delta G^\circ = -27.0$  kcal/mol and  $\Delta H^\circ = -74.3$  kcal/mol) are spontaneous, permitted by enthalpy and prohibited by entropy. **Figures 3** and **4** show that the formation of the species involved in the reaction mechanism (**C**, **TS1**, **I**, **TS2**, and **P**) is carried out by nonspontaneous reactions [except **P**(**3a**) for (i), and **C** and **P** for (ii) and (iii)] and prohibited by entropy. However, the formation of all the species in the reactions (ii) and (iii) is permitted by enthalpy (see **Figure 4**). Therefore,  $\text{ChCl}/\text{TsOH}$  and  $\text{ChCl}/\text{TsOH}/\text{H}_2\text{O}$  favor the enthalpy-driven binding of aniline to maleimide in the aza-Michael addition. The enthalpy-driven binding can be associated with a “cage effect” by the  $\text{ChCl}/\text{TsOH}$  and  $\text{ChCl}/\text{TsOH}/\text{H}_2\text{O}$  molecules that

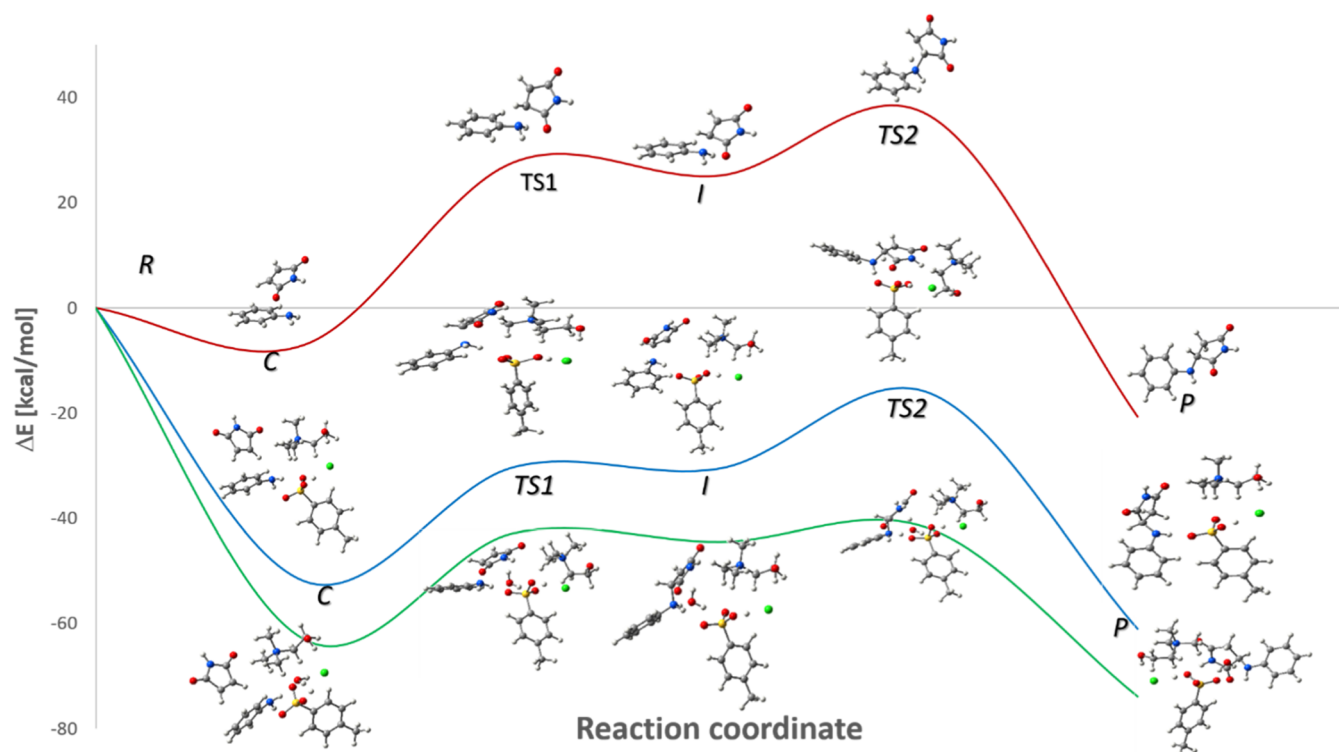
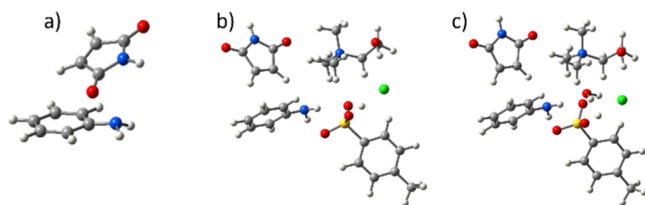
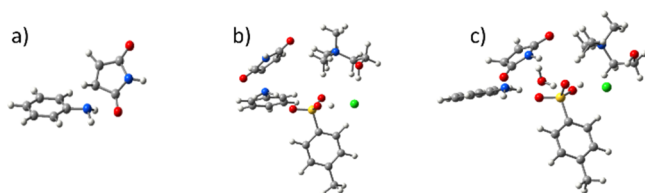


**Figure 2.** Energy profiles for the addition of 2a to 1. The red, blue, and green lines show the addition in the absence of molecules of the solvent and water and the presence of ChCl/TsOH and ChCl/TsOH/H<sub>2</sub>O, respectively. The relative electronic energies include zero-point energy corrections.

**Scheme 2. C** Obtained for the Addition of 2a to 1, (a) in the Absence of Molecules of the Solvent and Water, (b) in the Presence of ChCl/TsOH, and (c) in the Presence of ChCl/TsOH/H<sub>2</sub>O



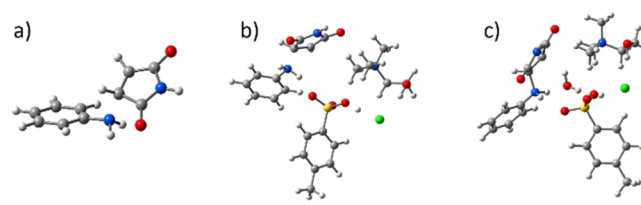
**Scheme 3. TS1** Obtained for the Addition of 2a to 1, (a) in the Absence of Molecules of the Solvent and Water, (b) in the Presence of ChCl/TsOH, and (c) in the Presence of ChCl/TsOH/H<sub>2</sub>O



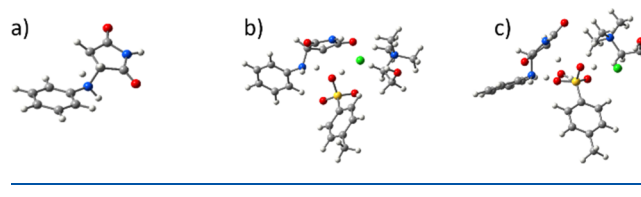
generate a transient dynamical confinement of the reagents and lead to a reduction in their degrees of freedom (spatial, orientation, and dynamic). The cage creates a “hole” that benefits the van der Waals interactions and hydrogen bonding between reagents and ChCl/TsOH or ChCl/TsOH/H<sub>2</sub>O.<sup>77,78</sup>

**2.5. Sixth Step: P → 3a + ChCl/TsOH (or ChCl/TsOH/H<sub>2</sub>O).** Following the Ruesgas-Ramón et al. suggestion for the extraction process,<sup>71</sup> we analyzed the affinity between the DES and the target compounds in terms of the disruption of P that

**Scheme 4. I** Obtained for the Addition of 2a to 1, (a) in the Absence of Molecules of Solvent and Water, (b) in the Presence of ChCl/TsOH, and (c) in the Presence of ChCl/TsOH/H<sub>2</sub>O



**Scheme 5. TS2** Obtained for the Addition of 2a to 1, (a) in the Absence of Molecules of the Solvent and Water, (b) in the Presence of ChCl/TsOH, and (c) in the Presence of ChCl/TsOH/H<sub>2</sub>O



releases 3a. For ChCl/TsOH/3a → ChCl/TsOH + 3a, the energy values were  $\Delta E = 1.9$  kcal/mol,  $\Delta G^\circ = -9.6$  kcal/mol,  $\Delta H^\circ = 0.8$  kcal/mol, and  $T\Delta S^\circ = 8.8$  kcal/mol, and for ChCl/TsOH/H<sub>2</sub>O/3a → ChCl/TsOH/H<sub>2</sub>O + 3a, the energy values were  $\Delta E = 3.4$  kcal/mol,  $\Delta G^\circ = -8.3$  kcal/mol,  $\Delta H^\circ = 2.3$  kcal/mol, and  $T\Delta S^\circ = 6.0$  kcal/mol. Therefore, the separation of 3a in both cases is spontaneous and is allowed by entropy. In the experiment, the DES (ChCl/TsOH) was recovered through evaporation of water, vacuum dried, and reused. The DES recyclability study revealed that this solvent can be used

Scheme 6. P Obtained for the Addition of 2a to 1, (a) in the Absence of Molecules of the Solvent and Water, (b) in the Presence of ChCl/TsOH, and (c) in the Presence of ChCl/TsOH/H<sub>2</sub>O

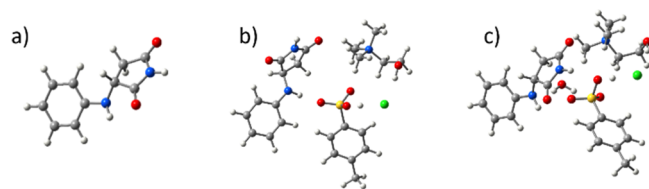


Table 3. Relative Energies for All the Species Involved in the Additions (i) 1 + 2a, (ii) 1 + 2a + ChCl + TsOH, and (iii) 1 + 2a + ChCl + TsOH + H<sub>2</sub>O<sup>a</sup>

species	(i) $\Delta E^b$ , $\Delta H^{oc}$ , $\Delta G^{oc}$ , $T\Delta S^{oc}$	(ii) $\Delta E^b$ , $\Delta H^{oc}$ , $\Delta G^{oc}$ , $T\Delta S^{oc}$	(iii) $\Delta E^b$ , $\Delta H^{oc}$ , $\Delta G^{oc}$ , $T\Delta S^{oc}$
R	0, 0, 0, 0	0, 0, 0, 0	0, 0, 0, 0
C	-7.0, -6.6, 3.6, -10.2	-51.9, -51.2, -16.3, -34.9	-63.0, -62.6, -18.5, -44.1
TS1	27.6, 26.8, 41.0, -14.2	-30.3, -29.9, 6.5, -36.4	-42.8, -43.3, 2.2, -45.5
I	25.2, 24.7, 38.1, -13.4	-30.4, -30.4, 8.7, -39.1	-44.5, -45.0, 0.9, -45.9
TS2	36.6, 35.9, 49.4, -13.5	-16.1, -16.1, 20.7, -36.8	-41.9, -43.4, 6.2, -49.6
P	-20.7, -21.2, -8.3, -12.9	-61.0, -60.4, -23.7, -36.7	-73.8, -74.3, -27.0, -47.3

<sup>a</sup>Values in kcal/mol. <sup>b</sup>The electronic energies including zero-point energy corrections. <sup>c</sup>The relative electronic energies, enthalpies, and Gibbs free energies values were obtained at  $T = 298.15$  K, and  $P = 1$  atm. The thermochemical values were computed at the M062X/6-311++G(d,p) level of theory using Gaussian09.

up to five reaction cycles without losing its activity (Figure 5). In the DES FT-IR spectra, no change between reaction cycles was observed.

It is interesting to observe that TS2 obtained in the fourth stage of the reaction mechanism involves a six-membered ring where the water molecule accepts a proton from the tetravalent nitrogen atom and donates a proton to the trivalent carbon atom; with this in mind, we carried out an H/D exchange NMR experiment to verify the presence of the deuterium atom in the carbon atom. Reaction 2a + 1 was performed first using ChCl/TsOH and then ChCl/TsOH/D<sub>2</sub>O. Reactions were stopped after 2 h, and product 3a was obtained for each reaction. Figure 6 shows the <sup>1</sup>H spectrum for the product 3a for both reactions (in CD<sub>3</sub>OD at room temperature). Interestingly, the methine resulting from the reaction after amine incorporation did not undergo deuterium addition (Figure 6), whereas the adjacent position was deuterated which indicates water proton addition in a regioselective process. Both the integrals of the signals and the appearance of the signals corroborated this. However, in order to support that the presence of deuterium in the product is not due to deuterium exchange with the maleimide under these conditions, the reaction was carried out in the presence of D<sub>2</sub>O, under the same reaction conditions, but without amine, resulting, as observed in the spectrum of <sup>1</sup>H NMR, in the absence of the deuterated product after 2 h of reaction.

The nature of the TS2 transition state was also verified through calculation of the intrinsic reaction coordinate<sup>79,80</sup> using the Gonzalez-Schlegel's method implemented in GAUSSIAN09<sup>73</sup> at the M062X/6-311++G(d,p) level of theory<sup>72</sup> (see the figures in the Supporting Information).

A final note, the analysis of the mole fractions of the reagents  $X_R$  (maleimide 1 + aniline 2a) and the DES  $X_{DES}$  (ChCl/TsOH), shows that in general  $X_R < X_{DES}$ , except for entries 3 and 4, where  $X_R > X_{DES}$  (see Table 4). Entries 3 and 4 display comparable numbers of "solute" as "solvent" molecules, and we observed that the entries had low yields of 3a (12 and 19%, respectively). The analysis including the mole fraction of water  $X_{H_2O}$  (entries 7–9) indicates that  $X_{H_2O} > X_{DES} > X_R$ . Although

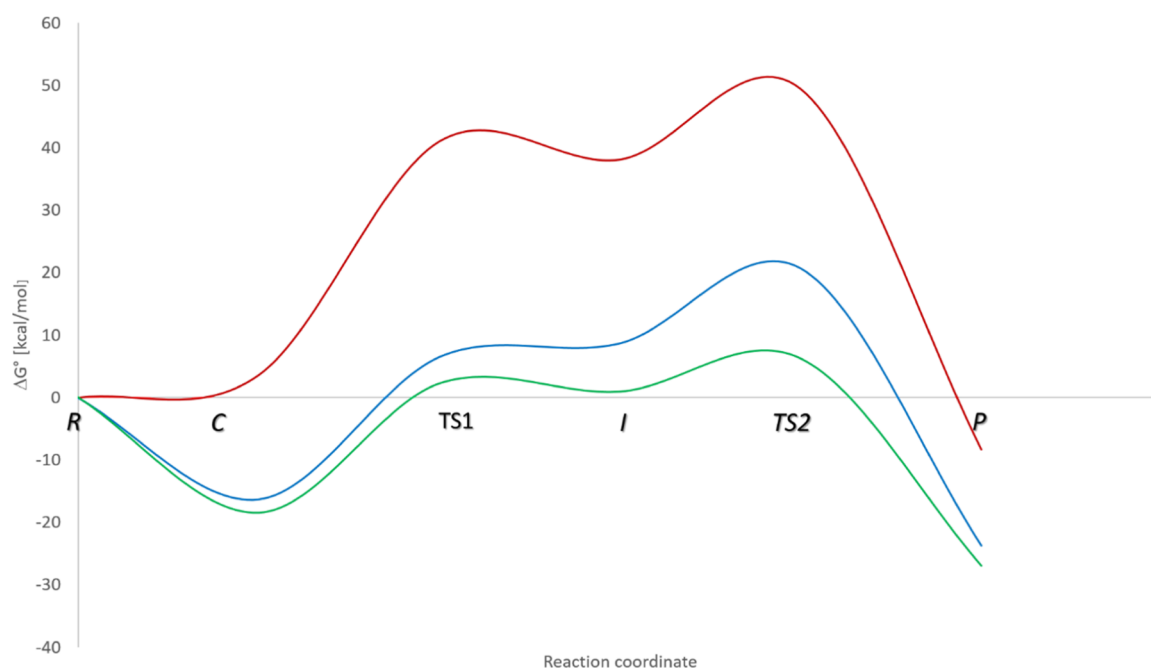
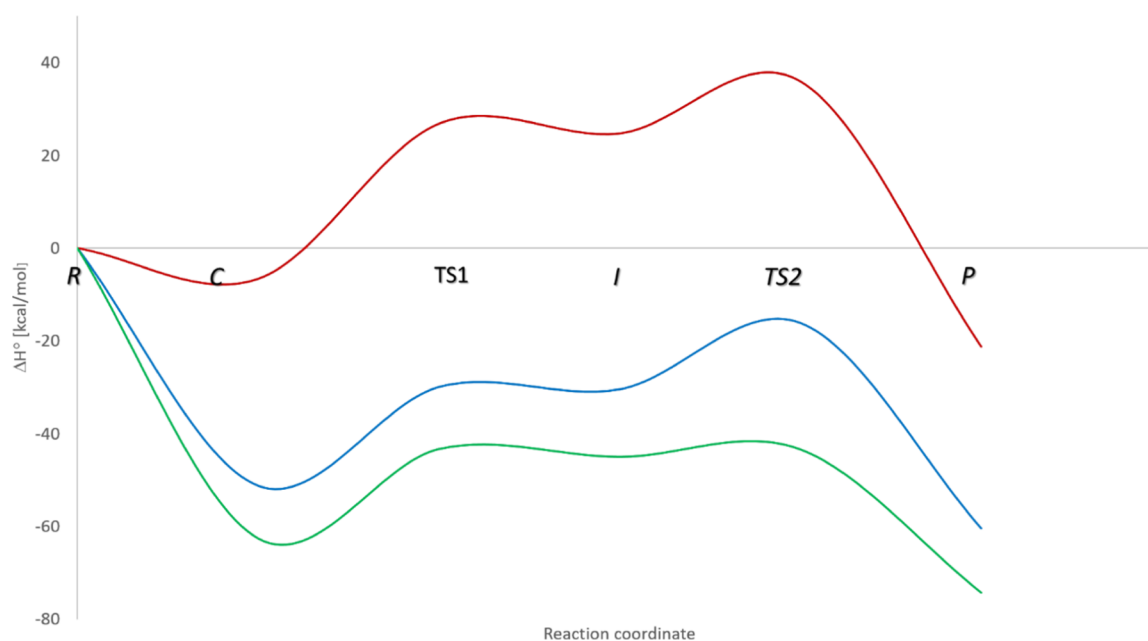
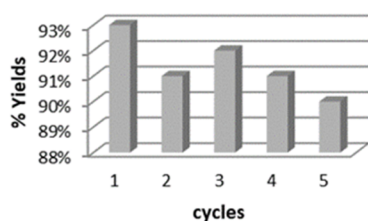


Figure 3. Gibbs free energy profiles for the addition of 2a to 1. The red, blue, and green lines show the addition in the absence of molecules of the solvent and water and the presence of ChCl/TsOH and ChCl/TsOH/H<sub>2</sub>O, respectively.



**Figure 4.** Enthalpy profiles for the addition of **2a** to **1**. The red, blue, and green lines show the addition in the absence of molecules of the solvent and water and the presence of ChCl/TsOH and ChCl/TsOH/H<sub>2</sub>O, respectively.



**Figure 5.** DES recyclability study.

the relationship between the yield of **3a** and  $X_{\text{H}_2\text{O}}$  is not linear ( $R^2 = 0.70$ ), the yield of **3a** increases when  $X_{\text{H}_2\text{O}}$  decreases. The experimental results showed that the higher yields of **3a** (see Table 1) were obtained with DES/H<sub>2</sub>O (93%, entry 7,  $X_{\text{DES}} = 0.155$ ,  $X_{\text{H}_2\text{O}} = 0.715$ , 50 °C and 1.5 h) and DES (82%, entry 6,  $X_{\text{DES}} = 0.545$ ,  $X_{\text{H}_2\text{O}} = 0$ , 90 °C, and 2 h). The water increased the yield of **3a** by 11% and decreased the time and temperature of the reaction by  $\Delta T = 40$  °C and  $\Delta t = 0.5$  h. According to the reaction mechanism, the rate-determining (rate-controlling) step of the reaction is the formation of TS1 (see Scheme 1 and Figure 2). Using the conventional transition theory,<sup>81,82</sup> we calculated the rate constant  $k$  for the reaction in the absence of DES and H<sub>2</sub>O (red line, Figure 2), the  $k_{(\text{DES})}$  for the reaction in the presence of DES (blue line, Figure 2), and the  $k_{(\text{DES}/\text{H}_2\text{O})}$  for the reaction in the presence of DES/H<sub>2</sub>O (green line, Figure 2). The ratio of reaction rates showed the trend  $\{[k_{(\text{DES}/\text{H}_2\text{O})}/k] = 28.998 \times 10^{11}\} > \{[k_{(\text{DES})}/k] = 2.305 \times 10^{11}\} \gg \{[k/k] = 1\}$ . Therefore, the transition state TS1 is stabilized to a greater extent with DESs and even more with DES/H<sub>2</sub>O.

### 3. CONCLUSIONS

We provided experimental and theoretical information about the structure of DES ChCl/TsOH, the kinetic and thermodynamic properties and interactions between the DES and the substrates anilines and maleimides in aza-Michael

addition, and the effect of water on the ChCl/TsOH supramolecular network and its physicochemical properties. We have developed an easy synthetic approach to obtain interesting varieties of pyrrolidinedione through the addition of aza-Michael of anilines to the maleimide in the DES ChCl/TsOH, which provides rapid access to the aminopyrrolidines-2,5-diones. This reaction, which generates the desired products, has the advantages such as a wide substrate range, high atom economy, and good tolerance to functional groups. The key to this reaction was to avoid the use of bases, metal catalysts, or ligands. The calculated potential energy surface for the addition of aniline to maleimide suggests a reaction mechanism of several steps. The energy profiles show that the reactions in the presence of ChCl/TsOH or ChCl/TsOH/H<sub>2</sub>O occur in the lowest energy curve, and all the species (complex, intermediate, transition states, and product) are more stable than the reagents. A set of H/D exchange NMR experiments validates the transition state existing in the fourth stage of the mechanism. The total reaction is exothermic, spontaneous, permitted by enthalpy, and prohibited for entropy. The relative stabilization by the enthalpy contributions (in kcal/mol) for TS1 and TS2 follows the trends  $(\delta\Delta^\ddagger H_{(\text{DES}/\text{H}_2\text{O})}^\circ = 70.1) > (\delta\Delta^\ddagger H_{(\text{DES})}^\circ = 56.7) > (\delta\Delta^\ddagger H^\circ = 0.0)$  and  $(\delta\Delta^\ddagger H_{(\text{DES}/\text{H}_2\text{O})}^\circ = 79.3) > (\delta\Delta^\ddagger H_{(\text{DES})}^\circ = 52.0) > (\delta\Delta^\ddagger H^\circ = 0.0)$ , respectively. The relative destabilization (in kcal/mol) by the entropy contributions for TS1 and TS2 follows the trends  $(\delta T\Delta^\ddagger S_{(\text{DES}/\text{H}_2\text{O})}^\circ = 31.3) > (\delta T\Delta^\ddagger S_{(\text{DES})}^\circ = 22.2) > (\delta T\Delta^\ddagger S^\circ = 0.0)$  and  $(\delta T\Delta^\ddagger S_{(\text{DES}/\text{H}_2\text{O})}^\circ = 36.1) > (\delta T\Delta^\ddagger S_{(\text{DES})}^\circ = 23.3) > (\delta T\Delta^\ddagger S^\circ = 0.0)$ , respectively. The relative stabilization by enthalpy contribution for TS1 and TS2 is twice the magnitude of the relative destabilization by enthalpy contribution (in kcal/mol) for TS1 and TS2. Therefore, ChCl/TsOH and the water incorporated in the supramolecular ChCl/TsOH complex increases the stabilization of TS1 and TS2 and favors the enthalpy-driven binding. The computational errors in this system using only one of the

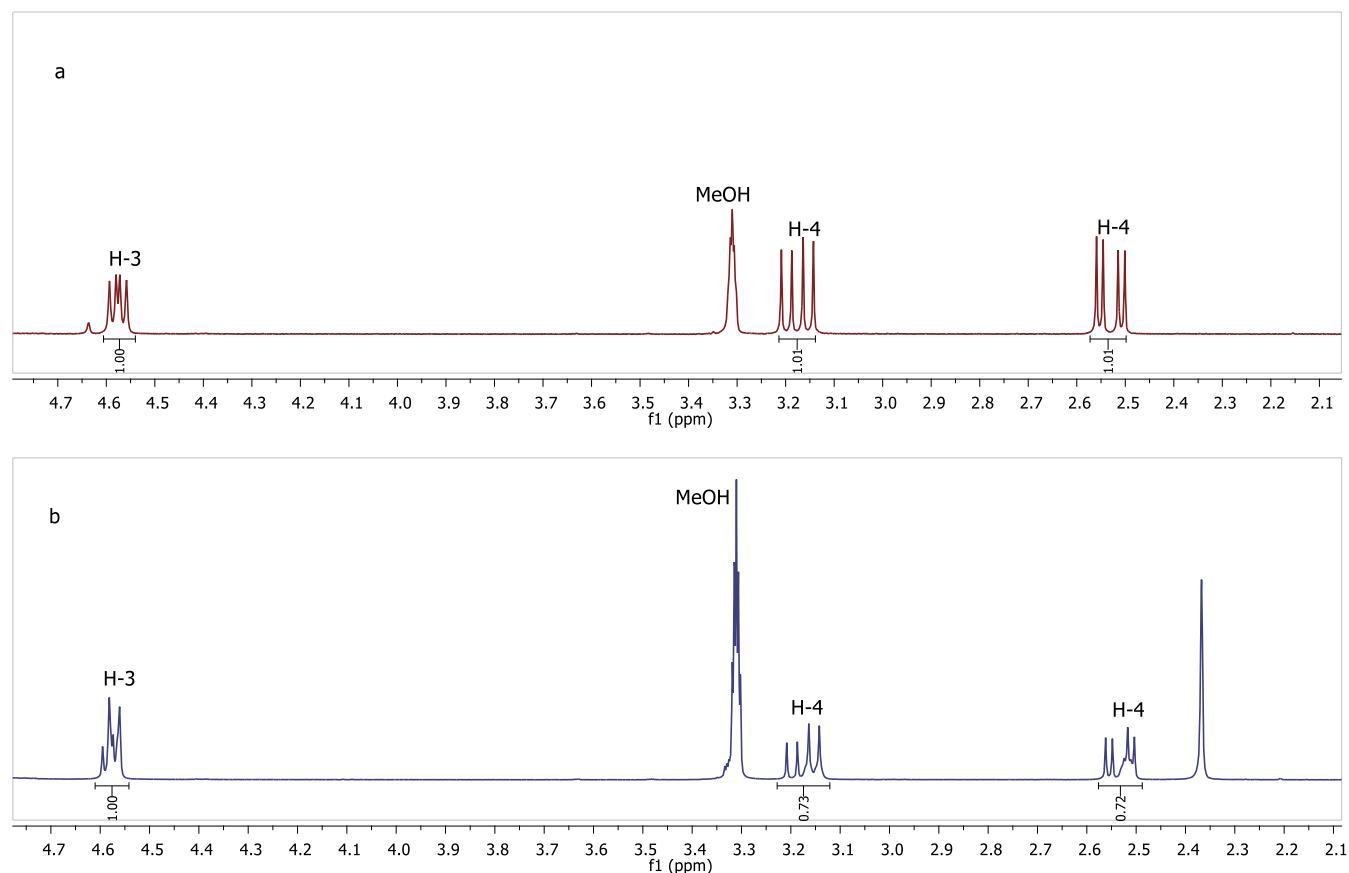
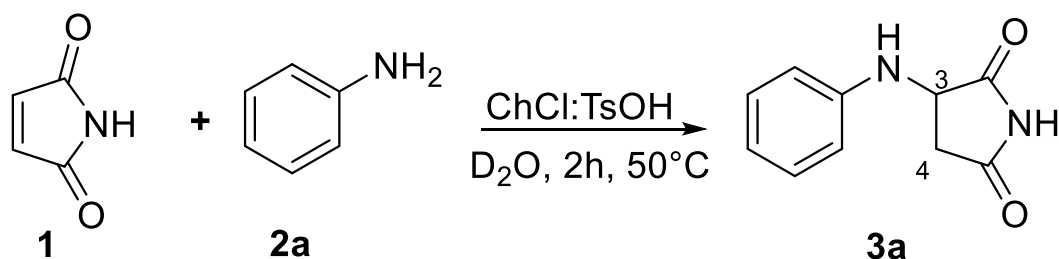


Figure 6. <sup>1</sup>H NMR (MeOH-*d*<sub>4</sub>) (a) using H<sub>2</sub>O in the reaction, (b) using D<sub>2</sub>O in the reaction.

Table 4. Mole Fractions of the Reagents, DESs, and Water

entry	$X_R$	$X_{DES}$	$X_{H_2O}$	$X_R/X_{DES}$	$X_R/(X_{DES} + X_{H_2O})$
1	0.36	0.64	0.00	0.56	0.56
2	0.45	0.55	0.00	0.83	0.83
3	0.53	0.47	0.00	1.11	1.11
4	0.63	0.38	0.00	1.67	1.67
5	0.45	0.55	0.00	0.83	0.83
6	0.45	0.55	0.00	0.83	0.83
7	0.13	0.16	0.72	0.83	0.15
8	0.13	0.16	0.72	0.83	0.15
9	0.05	0.06	0.89	0.83	0.05

molecules of the solvents ChCl, TsOH, and H<sub>2</sub>O should be not significant because the theoretical results are consistent with the experiments. However, we are working to introduce explicit solvents in the system and for generalization with other

reaction mechanisms (nucleophilic substitution and Diels–Alder reactions).

## 4. EXPERIMENTAL SECTION

**4.1. General Information.** Thin layer chromatography (TLC) analyses were performed on commercial aluminum plates bearing a 0.25 mm layer of Merck silica gel 60F254, which were visualized with UV light at 254 nm or under iodine. Column chromatography was performed with SiO<sub>2</sub> [F60 (230–400 mesh)]. High-resolution mass spectra (HRMS) were recorded on the MStation JMS-700 using electron impact (EI) ionization. GC/MS analysis were recorded on a Thermo Scientific ISQ LT Single Quadrupole Gas Chromatograph/Mass Spectrometer (GC/MS) using a TraceGOLD TG-SQC GC column (15 m × 0.25 mm × 0.25 μm) and an injection temperature of 240 °C, a detector temperature of 260 °C, an initial temperature of 50 °C for a 5 min hold, a final temperature of 250 °C for a 10 min hold, a flow rate of 1.0 mL/min, splitless, and a run time of 30 min. Infra-red (IR) spectra were recorded on a Thermo Scientific Nicolet

iS10 spectrometer using attenuated total reflection. Selected absorption maxima ( $\nu_{\max}$ ) are reported in wavenumbers ( $\text{cm}^{-1}$ ). Melting points were recorded in degrees Celsius ( $^{\circ}\text{C}$ ), using a Fisher–Johns melting point apparatus, and are reported uncorrected.  $^1\text{H}$  and  $^{13}\text{C}$   $\{^1\text{H}\}$  NMR spectra of solutions in  $\text{CD}_3\text{OD}$  and  $\text{DMSO}-d_6$  were recorded on a Mercury 400 spectrometer. Deuterated methanol and  $\text{DMSO}-d_6$  were used as received, and chemical shift values ( $\delta$ ) are reported in parts per million (ppm) relative to the residual signals of these solvents [ $\delta$  3.30 and 4.90 ppm for  $^1\text{H}$  ( $\text{CD}_3\text{OD}$ ) and  $\delta$  49.0 ppm for  $^{13}\text{C}$   $\{^1\text{H}\}$  ( $\text{CD}_3\text{OD}$ ) and  $\delta$  2.50 ppm for  $^1\text{H}$  ( $\text{DMSO}-d_6$ ) and  $\delta$  39.52 ppm for  $^{13}\text{C}$   $\{^1\text{H}\}$  ( $\text{DMSO}-d_6$ )]. Abbreviations used in the NMR follow-up experiments are as follows: s, singlet; d, doublet; t, triplet, and m, multiplet. The maleimide **1**, the arylamines **2a–2m**,  $\text{CHCl}_3$ , and  $\text{TsOH}$  were purchased from Sigma-Aldrich with purities more than 98%.  $\text{CHCl}_3$  was placed in an oven at  $100\text{ }^{\circ}\text{C}$  for 5 h to remove the water content. The other chemicals were used as received.

**4.2. Preparation of DESs ( $\text{CHCl}_3/\text{TsOH}$ ).** 1.8 mmol  $\text{CHCl}_3$  and 1.8 mmol  $\text{TsOH}$  were mixed in a 10 mL round-bottomed flask and heated in a sand bath on a hot plate magnetic stirrer for 15 min at  $120\text{ }^{\circ}\text{C}$  until a clear liquid appeared; the colorless liquid was used directly for the reactions without purification.

**4.3. Typical Procedure for the Aza-Michael Addition in  $\text{CHCl}_3/\text{pTsOH}$ .** 0.3 mL of water was added to  $\text{CHCl}_3/\text{TsOH}$  (0.59 g) with stirring for 5 min, and then, the maleimide **1** (0.097 g, 1 mmol) and aniline **2a** (0.19 g, 2 mmol) were slowly added to the reaction mixture. The reaction mixture was stirred at  $50\text{ }^{\circ}\text{C}$  in a sand bath on a hot plate magnetic stirrer for 1.5 h. The reaction was monitored by TLC. After completion of the reaction, water was added, an extraction was made with  $\text{AcOEt}$ , the organic phase was separated, and dried on anhydrous  $\text{MgSO}_4$ ; the solvent was evaporated under vacuum. The pure **3a** product was obtained by crystallization in methanol.

**4.4. Characterization Data of Compounds. 3-(Phenylamino)-pyrrolidine-2,5-dione **3a**.** According to the general procedure, the pure **3a** product was obtained by crystallization in methanol in 93% yield (0.176 g). Yellow pale solid, rf 0.42 (Hex/EtOAc 6:4), melting point (measured):  $177\text{--}179\text{ }^{\circ}\text{C}$ ;  $^1\text{H}$  NMR (400 MHz,  $\text{CD}_3\text{OD}$ ,  $\text{Me}_4\text{Si}$ ):  $\delta_{\text{H}}$  7.13–7.08 (m, 2H), 6.66 (dt,  $J = 7.2, 2.3$  Hz, 3H), 4.54 (dd,  $J = 8.5, 5.5$  Hz, 1H), 3.14 (dd,  $J = 17.9, 8.6$  Hz, 1H), 2.49 (dd,  $J = 17.9, 5.5$  Hz, 1H),  $^{13}\text{C}$   $\{^1\text{H}\}$  NMR (100 MHz,  $\text{CD}_3\text{OD}$ ;  $\text{Me}_4\text{Si}$ ):  $\delta_{\text{C}}$  180.6, 178.4, 148.5, 130.1, 119.2, 114.6, 54.9, 38.7; IR ( $\nu/\text{cm}^{-1}$ ): 3387, 1701, 1603, 1194, 753; HRMS (EI):  $m/z$  calcd for  $\text{C}_{10}\text{H}_{10}\text{N}_2\text{O}_3$ , 190.0742; found, 190.0745.

**4.5. 3-(*m*-Tolyl-amino)-pyrrolidine-2,5-dione **3b**.** According to the general procedure, **3b** was obtained by crystallization in methanol in 80% yield (0.164 g). Pink pale crystalline solid, rf 0.48 (Hex/EtOAc 6:4), melting point (measured):  $155\text{--}157\text{ }^{\circ}\text{C}$ ;  $^1\text{H}$  NMR (400 MHz,  $\text{CD}_3\text{OD}$ ;  $\text{Me}_4\text{Si}$ ):  $\delta_{\text{H}}$  7.01 (t,  $J = 7.9$  Hz, 1H), 6.52 (d,  $J = 5.3$  Hz, 2H), 6.48 (d,  $J = 8.1$  Hz, 1H), 4.54 (dd,  $J = 8.5, 5.5$  Hz, 1H), 3.15 (dd,  $J = 17.9, 8.6$  Hz, 1H), 2.51 (dd,  $J = 17.9, 5.5$  Hz, 1H), 2.23 (s, 3H);  $^{13}\text{C}$   $\{^1\text{H}\}$  NMR (100 MHz,  $\text{CD}_3\text{OD}$ ;  $\text{Me}_4\text{Si}$ ):  $\delta_{\text{C}}$  180.7, 178.4, 148.4, 139.9, 130.0, 120.2, 115.4, 111.8, 55.0, 38.8, 21.6; IR ( $\nu/\text{cm}^{-1}$ ): 3355, 1698, 1609, 1489, 1188, 765; HRMS (EI):  $m/z$  calcd for  $\text{C}_{11}\text{H}_{12}\text{N}_2\text{O}_3$ , 204.0899; found, 204.0899.

**4.6. 3-(*p*-Tolylamino)pyrrolidine-2,5-dione **3c**.** According to the general procedure, **3c** was obtained by crystallization in methanol in 86% yield (0.175 g). Pale yellow crystalline solid, rf 0.47 (Hex/EtOAc 6:4), melting point (measured):  $139\text{--}141\text{ }^{\circ}\text{C}$ ;  $^1\text{H}$  NMR (400 MHz,  $\text{CD}_3\text{OD}$ ;  $\text{Me}_4\text{Si}$ ):  $\delta_{\text{H}}$  6.96 (d,  $J = 8.5$  Hz, 2H), 6.60 (d,  $J = 8.4$ , 2H), 4.49 (dd,  $J = 8.5, 5.5$  Hz, 1H), 3.13 (dd,  $J = 17.9, 8.5$  Hz, 1H), 2.50 (dd,  $J = 17.9, 5.5$  Hz, 1H), 2.20 (s, 3H);  $^{13}\text{C}$   $\{^1\text{H}\}$  NMR (100 MHz,  $\text{CD}_3\text{OD}$ ;  $\text{Me}_4\text{Si}$ ):  $\delta_{\text{C}}$  180.7, 178.4, 146.0, 130.6, 128.6, 114.9, 55.3, 38.7, 20.5; IR ( $\nu/\text{cm}^{-1}$ ): 3390, 1704, 1615, 1521, 1197, 809.

**4.7. 3-((3-Hydroxyphenyl)amino)pyrrolidine-2,5-dione **3d**.** According to the general procedure and after purification on silica gel using a mixture of Hex/EtOAc (7:3, v/v) as the eluent, **3d** was obtained in 42% yield (0.087 g). Pale yellow solid, rf 0.17 (Hex/EtOAc 6:4), melting point (measured):  $168\text{--}171\text{ }^{\circ}\text{C}$ ;  $^1\text{H}$  NMR (400 MHz,  $\text{CD}_3\text{OD}$ ;  $\text{Me}_4\text{Si}$ ):  $\delta_{\text{H}}$  6.93 (t,  $J = 8.1$  Hz, 1H), 6.20–6.14 (m, 3H), 4.51 (dd,  $J = 8.3, 5.6$  Hz, 1H), 3.14 (dd,  $J = 17.9, 8.6$  Hz, 1H), 2.52 (dd,  $J = 17.9, 5.5$  Hz, 1H);  $^{13}\text{C}$   $\{^1\text{H}\}$  NMR (100 MHz,  $\text{CD}_3\text{OD}$ ;

$\text{Me}_4\text{Si}$ ):  $\delta_{\text{C}}$  180.6, 178.4, 159.3, 149.8, 130.9, 106.5, 101.6, 55.0, 38.8; IR ( $\nu/\text{cm}^{-1}$ ): 3383, 3172, 1693, 1603, 1192; HRMS (EI):  $m/z$  calcd for  $\text{C}_{10}\text{H}_{10}\text{N}_2\text{O}_3$ , 206.0691; found, 206.0702.

**4.8. 3-((4-Hydroxyphenyl)amino)pyrrolidine-2,5-dione **3e**.** According to the general procedure and after purification on silica gel using the mixture of Hex/EtOAc (7:3, v/v) as the eluent, **3e** was obtained in 27% yield (0.055 g). Dark green solid, rf 0.14 (Hex/EtOAc 6:4), melting point (measured)  $194\text{--}196\text{ }^{\circ}\text{C}$ ;  $^1\text{H}$  NMR (400 MHz,  $\text{CD}_3\text{OD}$ ;  $\text{Me}_4\text{Si}$ ):  $\delta_{\text{H}}$  6.64–6.57 (m, 4H), 4.41 (dd,  $J = 8.5, 5.4$  Hz, 1H), 3.09 (dd,  $J = 17.9, 8.5$  Hz, 1H), 2.48 (dd,  $J = 17.9, 5.4$  Hz, 1H);  $^{13}\text{C}$   $\{^1\text{H}\}$  NMR (100 MHz,  $\text{CD}_3\text{OD}$ ;  $\text{Me}_4\text{Si}$ ):  $\delta_{\text{C}}$  180.8, 178.5, 151.3, 141.2, 116.9, 56.2, 38.7; IR ( $\nu/\text{cm}^{-1}$ ): 3370, 3274, 1693, 1512; HRMS (EI):  $m/z$  calcd for  $\text{C}_{10}\text{H}_{10}\text{N}_2\text{O}_3$ , 206.0691; found, 206.0698.

**4.9. 3-((4-Chlorophenyl)amino)pyrrolidine-2,5-dione **3f**.** According to the general procedure, **3f** was obtained by crystallization in methanol in 84% yield (0.189 g). Pale yellow crystalline solid, rf 0.38 (Hex/EtOAc 6:4), melting point (measured)  $164\text{--}166\text{ }^{\circ}\text{C}$ ;  $^1\text{H}$  NMR (400 MHz,  $\text{CD}_3\text{OD}$ ;  $\text{Me}_4\text{Si}$ ):  $\delta_{\text{H}}$  7.07 (d,  $J = 8.9$  Hz, 2H), 6.64 (d,  $J = 8.8$  Hz, 2H), 4.52 (dd,  $J = 8.6, 5.5$  Hz, 1H), 3.14 (dd,  $J = 17.9, 8.6$  Hz, 1H), 2.49 (dd,  $J = 17.9, 5.5$  Hz, 1H);  $^{13}\text{C}$   $\{^1\text{H}\}$  NMR (100 MHz,  $\text{CD}_3\text{OD}$ ;  $\text{Me}_4\text{Si}$ ):  $\delta_{\text{C}}$  180.3, 178.2, 147.4, 129.9, 123.5, 115.6, 54.7, 38.6; IR ( $\nu/\text{cm}^{-1}$ ): 3387, 1704, 1599, 1486, 1170, 824.

**4.10. 3-((2-Bromophenyl)amino)pyrrolidine-2,5-dione **3g**.** According to the general procedure, **3g** was obtained by crystallization in EtOAc/methanol (6:4, v/v) in 43% yield (0.115 g). Pale orange crystalline solid, rf 0.54 (Hex/EtOAc 6:4), melting point (measured):  $149\text{--}152\text{ }^{\circ}\text{C}$ ;  $^1\text{H}$  NMR (400 MHz,  $\text{CD}_3\text{OD}$ ;  $\text{Me}_4\text{Si}$ ):  $\delta_{\text{H}}$  7.40 (dd,  $J = 7.9, 1.4$  Hz, 1H), 7.22–7.12 (m, 1H), 6.75 (dd,  $J = 8.1, 0.8$  Hz, 1H), 6.61 (td,  $J = 7.8, 1.4$  Hz, 1H), 4.64 (dd,  $J = 8.6, 5.9$  Hz, 1H), 3.20 (dd,  $J = 17.7, 8.6$  Hz, 1H), 2.59 (dd,  $J = 17.7, 5.9$  Hz, 1H);  $^{13}\text{C}$   $\{^1\text{H}\}$  NMR (100 MHz,  $\text{CD}_3\text{OD}$ ;  $\text{Me}_4\text{Si}$ ):  $\delta_{\text{C}}$  180.1, 178.0, 145.3, 133.7, 129.6, 120.1, 113.4, 110.8, 54.7, 38.9; IR ( $\nu/\text{cm}^{-1}$ ): 3373, 1701, 1592, 1486, 1188, 735; HRMS (EI):  $m/z$  calcd for  $\text{C}_{10}\text{H}_9\text{BrN}_2\text{O}_2$ , 267.9847; found, 267.9853 and  $m/z$   $[\text{M} + 2]$ , 269.9821.

**4.11. 3-((4-Iodophenyl)amino)pyrrolidine-2,5-dione **3h**.** According to the general procedure, **3h** was obtained by crystallization in EtOAc/methanol (6:4, v/v) in 91% yield (0.287 g). Colorless crystalline solid, rf 0.76 (Hex/EtOAc 6:4), melting point (measured):  $178\text{--}180\text{ }^{\circ}\text{C}$ ;  $^1\text{H}$  NMR (400 MHz,  $\text{CD}_3\text{OD}$ ;  $\text{Me}_4\text{Si}$ ):  $\delta_{\text{H}}$  7.36 (d,  $J = 8.8$  Hz, 2H), 6.50 (d,  $J = 8.8$  Hz, 2H), 4.52 (dd,  $J = 8.6, 5.5$  Hz, 1H), 3.14 (dd,  $J = 17.9, 8.6$  Hz, 1H), 2.48 (dd,  $J = 17.9, 5.5$  Hz, 1H);  $^{13}\text{C}$   $\{^1\text{H}\}$  NMR (100 MHz,  $\text{CD}_3\text{OD}$ ;  $\text{Me}_4\text{Si}$ ):  $\delta_{\text{C}}$  180.3, 178.1, 148.4, 138.8, 116.6, 79.1, 54.5, 38.5; IR ( $\nu/\text{cm}^{-1}$ ): 3328, 1783, 1692, 1588; HRMS (EI):  $m/z$  calcd for  $\text{C}_{10}\text{H}_9\text{IN}_2\text{O}_2$ , 315.9749; found, 315.9749.

**4.12. 3-((3,4-Dichlorophenyl)amino)pyrrolidine-2,5-dione **3i**.** According to the general procedure, **3i** was obtained by crystallization in methanol in 40% yield (0.104 g). Yellow crystalline solid, rf 0.38 (Hex/EtOAc 6:4), melting point (measured)  $192\text{--}194\text{ }^{\circ}\text{C}$ ;  $^1\text{H}$  NMR (400 MHz,  $\text{CD}_3\text{OD}$ ;  $\text{Me}_4\text{Si}$ ):  $\delta_{\text{H}}$  7.19 (d,  $J = 8.8$  Hz, 1H), 6.84 (d,  $J = 2.7$  Hz, 1H), 6.61 (dd,  $J = 8.8, 2.7$  Hz, 1H), 4.56 (dd,  $J = 8.7, 5.5$  Hz, 1H), 3.17 (dd,  $J = 17.9, 8.7$  Hz, 1H), 2.50 (dd,  $J = 17.9, 5.5$  Hz, 1H);  $^{13}\text{C}$   $\{^1\text{H}\}$  NMR (100 MHz,  $\text{CD}_3\text{OD}$ ;  $\text{Me}_4\text{Si}$ ):  $\delta_{\text{C}}$  180.1, 178.0, 148.7, 133.5, 131.6, 120.9, 115.4, 114.2, 54.4, 38.4; IR ( $\nu/\text{cm}^{-1}$ ): 3367, 1689, 1595, 1471, 856, 800; HRMS (EI):  $m/z$  calcd for  $\text{C}_{10}\text{H}_8\text{Cl}_2\text{N}_2\text{O}_2$ , 257.9963; found, 257.9975.

**4.13. 3-((4-Benzoylphenyl)amino)pyrrolidine-2,5-dione **3j**.** According to the general procedure and after purification on silica gel using the mixture of Hex/EtOAc (7:3, v/v) as the eluent, **3j** was obtained in 80% yield (0.236 g). Yellow solid, rf 0.19 (Hex/EtOAc 6:4), melting point (measured)  $180\text{--}183\text{ }^{\circ}\text{C}$ ;  $^1\text{H}$  NMR (400 MHz,  $\text{CD}_3\text{OD}$ ;  $\text{Me}_4\text{Si}$ ):  $\delta_{\text{H}}$  7.65 (t,  $J = 8.2$  Hz, 4H), 7.56 (t,  $J = 7.4$  Hz, 1H), 7.47 (t,  $J = 7.7$  Hz, 2H), 6.74 (d,  $J = 8.6$  Hz, 2H), 4.74 (dd,  $J = 8.4, 5.8$  Hz, 1H), 3.21 (dd,  $J = 17.9, 8.8$  Hz, 1H), 2.57 (dd,  $J = 17.9, 5.6$  Hz, 1H);  $^{13}\text{C}$   $\{^1\text{H}\}$  NMR (100 MHz,  $\text{CD}_3\text{OD}$ ;  $\text{Me}_4\text{Si}$ ):  $\delta_{\text{C}}$  197.5, 179.7, 177.8, 153.5, 140.1, 134.0, 132.7, 130.4, 129.2, 127.2, 113.0, 53.9, 38.3; IR ( $\nu/\text{cm}^{-1}$ ): 3324, 1704, 1592, 1558, 1318, 1279, 1191, 1143; HRMS (EI):  $m/z$  calcd for  $\text{C}_{17}\text{H}_{14}\text{N}_2\text{O}_3$ , 294.1004; found, 294.1023.

**4.14. 3-((3-Nitrophenyl)amino)pyrrolidine-2,5-dione **3k**.** According to the general procedure and after purification on silica gel

using the mixture of Hex/EtOAc (7:3, v/v) as the eluent, **3k** was obtained in 57% yield (0.133 g). Yellow powder, rf 0.28 (Hex/EtOAc 6:4), melting point (measured) 175–177 °C; <sup>1</sup>H NMR (400 MHz, CD<sub>3</sub>OD; Me<sub>4</sub>Si): δ<sub>H</sub> 7.53 (t, *J* = 2.3 Hz, 1H), 7.49 (ddd, *J* = 8.1, 2.1, 0.8 Hz, 1H), 7.31 (t, *J* = 8.1 Hz, 1H), 7.07–7.04 (m, 1H), 4.70 (dd, *J* = 8.7, 5.5 Hz, 1H), 3.21 (dd, *J* = 17.9, 8.8 Hz, 1H), 2.55 (dd, *J* = 17.9, 5.5 Hz, 1H); <sup>13</sup>C {<sup>1</sup>H} NMR (100 MHz, CD<sub>3</sub>OD; Me<sub>4</sub>Si): δ<sub>C</sub> 180.0, 177.9, 150.7, 150.0, 130.9, 120.1, 113.0, 107.9, 54.3, 38.3; IR (ν/cm<sup>-1</sup>): 3353, 1688, 1541, 1343, 1263, 1160, 734; HRMS (EI): *m/z* calcd for C<sub>10</sub>H<sub>9</sub>N<sub>3</sub>O<sub>4</sub>, 235.0593; found, 235.0602.

**4.15. 3-(2-Nitrophenyl)amino)pyrrolidine-2,5-dione 3l.** According to the general procedure, **3l** was obtained by crystallization in EtOAc/methanol (6:4, v/v) in 37% yield (0.088 g). Orange crystal, rf 0.34 (Hex/EtOAc 6:4), melting point (measured) 191–194 °C; <sup>1</sup>H NMR (400 MHz, DMSO-*d*<sub>6</sub>; Me<sub>4</sub>Si): δ<sub>H</sub> 11.39 (s, 1H), 8.36 (d, *J* = 8.1 Hz, 1H), 8.08 (dd, *J* = 8.6, 1.5 Hz, 1H), 7.59–7.53 (m, 1H), 7.13 (d, *J* = 8.6 Hz, 1H), 6.80–6.73 (m, 1H), 5.04 (dt, *J* = 8.4, 6.4 Hz, 1H), 3.13 (dd, *J* = 17.2, 8.8 Hz, 1H), 2.71 (dd, *J* = 17.2, 6.2 Hz, 1H); <sup>13</sup>C {<sup>1</sup>H} NMR (100 MHz, DMSO-*d*<sub>6</sub>; Me<sub>4</sub>Si): δ<sub>C</sub> 177.8, 175.9, 144.2, 136.5, 131.8, 126.2, 116.3, 114.9, 52.2, 37.3; IR (ν/cm<sup>-1</sup>): 3356, 1710, 1616, 1510.

**4.16. 3-(Methyl(phenyl)amino)pyrrolidine-2,5-dione 3m.** According to the general procedure, **3m** was obtained by crystallization in methanol in 90% yield (0.184 g). Colorless crystalline solid, rf 0.43 (Hex/EtOAc 6:4), melting point (measured) 165–167 °C; <sup>1</sup>H NMR (400 MHz, CD<sub>3</sub>OD; Me<sub>4</sub>Si): δ<sub>H</sub> 7.20 (dd, *J* = 8.8, 7.3 Hz, 2H), 6.86 (d, *J* = 8 Hz, 2H), 6.75 (t, *J* = 7.3 Hz, 1H), 5.08 (dd, *J* = 9, 5.9 Hz, 1H), 3.01 (dd, *J* = 18.2, 9 Hz, 1H), 2.81 (s, 3H), 2.71 (dd, *J* = 18.2, 5.9 Hz, 1H); <sup>13</sup>C {<sup>1</sup>H} NMR (100 MHz, CD<sub>3</sub>OD; Me<sub>4</sub>Si): δ<sub>C</sub> 179.8, 178.0, 150.8, 130.2, 119.6, 115.3, 61.7, 34.3, 33.8; IR (ν/cm<sup>-1</sup>): 3196, 1689, 1598, 1495, 1241, 759, 694; HRMS (EI): *m/z* calcd for C<sub>11</sub>H<sub>12</sub>N<sub>2</sub>O<sub>2</sub>, 204.0899; found, 204.0904.

## ■ ASSOCIATED CONTENT

### Supporting Information

The Supporting Information is available free of charge at <https://pubs.acs.org/doi/10.1021/acs.joc.0c02039>.

Experimental procedures; compound characterization data and spectra; and details of calculation (PDF)

## ■ AUTHOR INFORMATION

### Corresponding Authors

Francisco Méndez – Departamento de Química, División de Ciencias Básicas e Ingeniería, Universidad Autónoma Metropolitana-Iztapalapa, México D. F. 09340, Mexico; Loire Valley Institute for Advanced Studies, Orléans & Tours, France CEMHTI, Orléans 45000, France; [orcid.org/0000-0002-0555-1528](https://orcid.org/0000-0002-0555-1528); Email: [fm@xanum.uam.mx](mailto:fm@xanum.uam.mx)

Claudia Araceli Contreras-Celedón – Departamento de Síntesis Orgánica, Instituto de Investigaciones Químico Biológicas, Universidad Michoacana de San Nicolás de Hidalgo, Morelia 58030, Michoacán, Mexico; Email: [celedon@umich.mx](mailto:celedon@umich.mx)

### Authors

Abelardo Gutiérrez-Hernández – Departamento de Síntesis Orgánica, Instituto de Investigaciones Químico Biológicas, Universidad Michoacana de San Nicolás de Hidalgo, Morelia 58030, Michoacán, Mexico

Arlette Richaud – Departamento de Química, División de Ciencias Básicas e Ingeniería, Universidad Autónoma Metropolitana-Iztapalapa, México D. F. 09340, Mexico; Loire Valley Institute for Advanced Studies, Orléans & Tours, France CEMHTI, Orléans 45000, France

Luis Chacón-García – Departamento de Síntesis Orgánica, Instituto de Investigaciones Químico Biológicas, Universidad

Michoacana de San Nicolás de Hidalgo, Morelia 58030, Michoacán, Mexico

Carlos J. Cortés-García – Departamento de Síntesis Orgánica, Instituto de Investigaciones Químico Biológicas, Universidad Michoacana de San Nicolás de Hidalgo, Morelia 58030, Michoacán, Mexico

Complete contact information is available at: <https://pubs.acs.org/10.1021/acs.joc.0c02039>

## Author Contributions

C.A.C.-C. conceived and designed the experiments and wrote the first draft of the paper; A.G.-H and C.A.C.-C. carried out the experimental work and provided reagents, materials, and analysis tools; C.A.C.-C., L.C.-G., and C.J.C.-G. analyzed the data and participated in the discussion of the obtained experimental results; A.R. and F.M. carried out the calculations and analyzed the theoretical results. F.M. conceived and designed the theoretical work and wrote the last draft of the document, and all the authors participated in its revision. All authors have read and accepted the published version of the manuscript.

## Notes

The authors declare no competing financial interest.

## ■ ACKNOWLEDGMENTS

C.A.C.-C. thanks the CIC-UMSNH for financial support of this project, A.G.-H. thanks CONACyT (grant no. 922285) for a graduate fellowship. A.R. thanks LE STUDIUM, Loire Valley Institute for Advanced Studies, Orléans & Tours, France, and the research fellow and funding from the European Union's Horizon 2020 research and innovation program under the Marie Skłodowska-Curie grant agreement no. 665790. F.M. thanks Programa Especial de Apoyo a la investigación básica UAM-2019.

## ■ DEDICATION

This work is dedicated to Prof. Virgilio Mendoza-García who introduced us to aza-Michael addition.

## ■ REFERENCES

- (1) Sheldon, R. A. The E factor 25 years on: the rise of green chemistry and sustainability. *Green Chem.* **2017**, *19*, 18–43.
- (2) Li, C.-J.; Trost, B. M. Green chemistry for chemical synthesis. *Proc. Natl. Acad. Sci. U.S.A.* **2008**, *105*, 13197–13202.
- (3) Clarke, C. J.; Tu, W.-C.; Levers, O.; Bröhl, A.; Hallett, J. P. Green and Sustainable Solvents in Chemical Processes. *Chem. Rev.* **2018**, *118*, 747–800.
- (4) Kralisch, D.; Ott, D.; Gericke, D. Rules and benefits of Life Cycle Assessment in green chemical process and synthesis design: a tutorial review. *Green Chem.* **2015**, *17*, 123–145.
- (5) Blaser, H.-U.; Studer, M. Catalysis for fine chemicals: who needs (will use) new solvents? *Green Chem.* **2003**, *5*, 112–117.
- (6) Shin, H.-M.; McKone, T. E.; Bennett, D. H. Contribution of low vapor pressure-volatile organic compounds (LVPVOCs) from consumer products to ozone formation in urban atmospheres. *Atmos. Environ.* **2015**, *108*, 98–106.
- (7) Henderson, R. K.; Jiménez-González, C.; Constable, D. J. C.; Alston, S. R.; Inglis, G. G. A.; Fisher, G.; Sherwood, J.; Binks, S. P.; Curzons, A. D. Expanding GSK's solvent selection guide – embedding sustainability into solvent selection starting at medicinal chemistry. *Green Chem.* **2011**, *13*, 854–862.
- (8) Wilkes, J. S. A short history of ionic liquids—from molten salts to neoteric solvents. *Green Chem.* **2002**, *4*, 73–80.

- (9) Vaddula, B. R.; Yalla, S.; González, M. A. Opportunities for the Replacement/Minimization of Selective Hazardous Solvents: Applications, Concerns and Approaches to Identify Alternatives. *Green Technologies for the Environment*; ACS Symposium Series; American Chemical Society, 2014; Vol. 1186, Chapter 5, pp 69–113.
- (10) Subramaniam, B. Exploiting Neoteric Solvents for Sustainable Catalysis and Reaction Engineering: Opportunities and Challenges. *Ind. Eng. Chem. Res.* **2010**, *49*, 10218–10229.
- (11) Reichardt, C. Solvents and Solvent Effects: An Introduction. *Org. Process Res. Dev.* **2007**, *11*, 105–113.
- (12) Tang, B.; Row, K. H. Recent developments in deep eutectic solvents in chemical sciences. *Monatsh. Chem.* **2013**, *144*, 1427–1454.
- (13) Florindo, C.; Oliveira, F. S.; Rebelo, L. P. N.; Fernandes, A. M.; Marrucho, I. M. Insights into the Synthesis and Properties of Deep Eutectic Solvents Based on Cholinium Chloride and Carboxylic. *Sustain. Chem. Eng.* **2014**, *2*, 2416–2425.
- (14) Abbott, A. P.; Capper, G.; Davies, D. L.; Rasheed, R. K.; Tambyrajah, V. Novel solvent properties of choline chloride/urea mixtures. *Chem. Commun.* **2003**, 70–71.
- (15) Abbott, A. P.; Boothby, D.; Capper, G.; Davies, D. L.; Rasheed, R. K. Deep Eutectic Solvents Formed between Choline Chloride and Carboxylic Acids: Versatile Alternatives to Ionic Liquids. *J. Am. Chem. Soc.* **2004**, *126*, 9142–9147.
- (16) Smith, E. L.; Abbott, A. P.; Ryder, K. S. Deep Eutectic Solvents (DESs) and Their Applications. *Chem. Rev.* **2014**, *114*, 11060–11082.
- (17) Francisco, M.; van den Bruinhorst, A.; Kroon, M. C. Low-Transition-Temperature Mixtures (LTTMs): A New Generation of Designer Solvents. *Angew. Chem., Int. Ed.* **2013**, *52*, 3074–3085.
- (18) Ruß, C.; König, B. Low melting mixtures in organic synthesis – an alternative to ionic liquids? *Green Chem.* **2012**, *14*, 2969–2982.
- (19) Hayyan, M.; Hashim, M. A.; Hayyan, A.; Al-Saadi, M. A.; AlNashef, I. M.; Mirghani, M. E. S.; Saheed, O. K. Are deep eutectic solvents benign or toxic? *Chemosphere* **2013**, *90*, 2193–2195.
- (20) Radošević, K.; Cvjetko Bubalo, M.; Gaurina Srček, V.; Grgas, D.; Landeka Dragičević, T.; Radojčić Redovniković, I. Evaluation of toxicity and biodegradability of choline chloride based deep eutectic solvents. *Ecotoxicol. Environ. Saf.* **2015**, *112*, 46–53.
- (21) Juneidi, I.; Hayyan, M.; Hashim, M. A. Evaluation of toxicity and biodegradability for cholinium-based deep eutectic solvents. *RSC Adv.* **2015**, *5*, 83636–83647.
- (22) Shahbaz, K.; Mjalli, F. S.; Hashim, M. A.; AlNashef, I. M. Prediction of deep eutectic solvents densities at different temperatures. *Thermochim. Acta* **2011**, *515*, 67–72.
- (23) El Achkar, T.; Fourmentin, S.; Greige-Gerges, H. Deep eutectic solvents: An overview on their interactions with water and biochemical compounds. *J. Mol. Liq.* **2019**, *288*, 111028.
- (24) Vilková, M.; Plotka-Wasyłka, J.; Andruch, V. The role of water in deep eutectic solvent-base extraction. *J. Mol. Liq.* **2020**, *304*, 112747.
- (25) Ma, C.; Laaksonen, A.; Liu, C.; Lu, X.; Ji, X. The peculiar effect of water on ionic liquids and deep eutectic solvents. *Chem. Soc. Rev.* **2018**, *47*, 8685–8720.
- (26) D'Agostino, C.; Gladden, L. F.; Mantle, M. D.; Abbott, A. P.; Ahmed, E. I.; Al-Murshedi, A. Y. M.; Harris, R. C. Molecular and ionic diffusion in aqueous – deep eutectic solvent mixtures: probing intermolecular interactions using PFG NMR. *Phys. Chem. Chem. Phys.* **2015**, *17*, 15297–15304.
- (27) López-Salas, N.; Vicent-Luna, J. M.; Imberti, S.; Posada, E.; Roldán, M. J.; Anta, J. A.; Balestra, S. R. G.; Madero Castro, R. M.; Calero, S.; Jiménez-Riobóo, R. J.; Gutiérrez, M. C.; Ferrer, M. L.; del Monte, F. Looking at the “Water-in-Deep-Eutectic-Solvent” System: A Dilution Range for High Performance Eutectics. *ACS Sustainable Chem. Eng.* **2019**, *7*, 17565–17573.
- (28) Fetisov, E. O.; Harwood, D. B.; Kuo, I.-F. W.; Warrag, S. E. E.; Kroon, M. C.; Peters, C. J.; Siepmann, J. I. First-Principles Molecular Dynamics Study of a Deep Eutectic Solvent: Choline Chloride/Urea and Its Mixture with Water. *J. Phys. Chem. B* **2018**, *122*, 1245–1254.
- (29) Kumari, P.; Shobhna, S.; Kaur, H. K. Influence of Hydration on the Structure of Reline Deep Eutectic Solvent: A Molecular Dynamics Study. *ACS Omega* **2018**, *3*, 15246–15255.
- (30) Tomé, L. I. N.; Baião, V.; da Silva, W.; Brett, C. M. A. Deep eutectic solvents for the production and application of new materials. *Appl. Mater. Today* **2018**, *10*, 30–50.
- (31) Mbous, Y. P.; Hayyan, M.; Hayyan, A.; Wong, W. F.; Hashim, M. A.; Looi, C. Y. Applications of deep eutectic solvents in biotechnology and bioengineering—Promises and challenges. *Biotechnol. Adv.* **2017**, *35*, 105–134.
- (32) Alonso, D. A.; Baeza, A.; Chinchilla, R.; Guillena, G.; Pastor, I. M.; Ramón, D. J. Deep Eutectic Solvents: The Organic Reaction Medium of the Century. *Eur. J. Org. Chem.* **2016**, 612–632.
- (33) Zhang, Q.; De Oliveira Vigier, K.; Royer, S.; Jérôme, F. Deep eutectic solvents: syntheses, properties and applications. *Chem. Soc. Rev.* **2012**, *41*, 7108–7146.
- (34) Liu, P.; Hao, J.-W.; Mo, L.-P.; Zhang, Z.-H. Recent advances in the application of deep eutectic solvents as sustainable media as well as catalysts in organic reactions. *RSC Adv.* **2015**, *5*, 48675–48704.
- (35) Gholami, S.; Roosta, A. Experimental Study and Modelling of Bubble Point of Aqueous Mixtures of Deep Eutectic Solvents Based on Dicarboxylic Acids and Choline Chloride. *J. Chem. Eng. Data* **2020**, *65*, 2743–2750.
- (36) Tajmir, F.; Roosta, A. Solubility of cefixime in aqueous mixtures of deep eutectic solvents from experimental study and modelling. *J. Mol. Liq.* **2020**, *303*, 112636.
- (37) Gholami, S.; Roosta, A. Bubble point of aqueous mixtures of sugar-based deep eutectic solvents and their individual components: Experimental study and modelling. *J. Mol. Liq.* **2019**, *296*, 111876.
- (38) Mohgimi, M.; Roosta, A. Physical properties of aqueous mixtures of (choline chloride + glucose) deep eutectic solvents. *J. Chem. Thermodyn.* **2019**, *129*, 159–165.
- (39) Martins, M. A. R.; Pinho, S. P.; Coutinho, J. A. P. Insights into the Nature of Eutectic and Deep Eutectic Mixtures. *J. Solution Chem.* **2019**, *48*, 962–982.
- (40) Araujo, C. F.; Coutinho, J. A. P.; Nolasco, M. M.; Parker, S. F.; Ribeiro-Claro, P. J. A.; Rudić, S.; Soares, B. I. G.; Vaz, P. D. Inelastic neutron scattering study of reline: shedding light on the hydrogen bonding network of deep eutectic solvents. *Phys. Chem. Chem. Phys.* **2017**, *19*, 17998.
- (41) Perkins, S. L.; Painter, P.; Colina, C. M. Experimental and Computational Studies of Choline Chloride-Based Deep Eutectic Solvents. *J. Chem. Eng. Data* **2014**, *59*, 3652–3662.
- (42) Rimsza, J. M.; Corrales, L. R. Adsorption complexes of copper and copper oxide in the deep eutectic solvent 2:1 urea–choline chloride. *Comput. Theor. Chem.* **2012**, *987*, 57–61.
- (43) Perkins, S. L.; Painter, P.; Colina, C. M. Molecular Dynamic Simulations and Vibrational Analysis of an Ionic Liquid Analogue. *J. Phys. Chem. B* **2013**, *117*, 10250–10260.
- (44) Sun, H.; Li, Y.; Wu, X.; Li, G. Theoretical study on the structures and properties of mixtures of urea and choline chloride. *J. Mol. Model.* **2013**, *19*, 2433–2441.
- (45) Brière, J.-F.; Charpentier, P.; Dupas, G.; Quéguiner, G.; Bourguignon, J. Regioselective Reductions of Various 3-Amino-succinimides; Application to the Synthesis of two Heterocyclic Systems. *Tetrahedron* **1997**, *53*, 2075–2086.
- (46) Klaene, J. J.; Ni, W.; Alfaro, J. F.; Zhou, Z. S. Detection and Quantitation of Succinimide in Intact Protein via Hydrazine Trapping and Chemical Derivatization. *J. Pharm. Sci.* **2014**, *103*, 3033–3042.
- (47) Desfougères, Y.; Jardin, J.; Lechevalier, V.; Pezennec, S.; Nau, F. Succinimidyl Residue Formation in Hen Egg-White Lysozyme Favors the Formation of Intermolecular Covalent Bonds without Affecting Its Tertiary Structure. *Biomacromolecules* **2011**, *12*, 156–166.
- (48) Nadimpally, K. C.; Paul, A.; Mandal, B. Reversal of Aggregation Using  $\beta$ -Breaker Dipeptide Containing Peptides : Application to  $A\beta(1-40)$  Self-Assembly and Its Inhibition. *ACS Chem. Neurosci.* **2014**, *5*, 400–408.

- (49) Wang, P.; Aussedat, B.; Vohra, Y.; Danishefsky, S. J. An Advance in the Chemical Synthesis of Homogeneous N-Linked Glycopolypeptides by Convergent Aspartylation. *Angew. Chem., Int. Ed.* **2012**, *51*, 11571–11575.
- (50) Cvetković, J. P.; Božić, B. Đ.; Banjac, N. R.; Petrović, J.; Soković, M.; Vitnik, V. D.; Vitnik, Z. J.; Ušćumlić, G. S.; Valentić, N. V. Synthesis, antimicrobial activity and quantum chemical investigation of novel succinimide derivatives. *J. Mol. Struct.* **2019**, *1181*, 148–156.
- (51) Firke, S. D.; Bari, S. B. Synthesis, biological evaluation and docking study of maleimide derivatives bearing benzenesulfonamide as selective COX-2 inhibitors and anti-inflammatory agents. *Bioorg. Med. Chem.* **2015**, *23*, 5273–5281.
- (52) Dall, E.; Fegg, J. C.; Briza, P.; Brandstetter, H. Structure and Mechanism of an Aspartimide-Dependent Peptide Ligase in Human Legumain. *Angew. Chem., Int. Ed.* **2015**, *54*, 2917–2921.
- (53) Panov, A. A.; Simonov, A. Y.; Lavrenov, S. N.; Lakatosh, S. A.; Trenin, A. S. 3,4-Disubstituted maleimides: synthesis and biological activity. *Chem. Heterocycl. Compd.* **2018**, *54*, 103–113.
- (54) Méndez, F.; Galván, M. Nucleophilic attacks on maleic anhydride: a density functional theory approach. In *Density Functional Methods in Chemistry*; Lebanowski, J. K., Andzelm, J. W., Eds.; Springer: New York, 1991; pp 387–400.
- (55) Méndez, F.; Galván, M.; Garritz, A.; Vela, A.; Gàzquez, J. Local softness and chemical reactivity of maleimide: nucleophilic addition. *J. Mol. Struct.: THEOCHEM* **1992**, *277*, 81–86.
- (56) Méndez, F.; Gàzquez, J. L. Chemical Reactivity of Enolate Ions: The Local Hard and Soft Acids and Bases Principle Viewpoint. *J. Am. Chem. Soc.* **1994**, *116*, 9298–9301.
- (57) Pearson, R. G. Hard and Soft Acids and Bases. *J. Am. Chem. Soc.* **1963**, *85*, 3533–3539.
- (58) Parr, R. G.; Yang, W. *Density Functional Theory of Atoms and Molecules*; Oxford University Press: New York, 1989.
- (59) Parr, R. G.; Pearson, R. G. Absolute hardness: companion parameter to absolute electronegativity. *J. Am. Chem. Soc.* **1983**, *105*, 7512–7516.
- (60) Gàzquez, J. L.; Méndez, F. The Hard and Soft Acids and Bases Principle: An Atoms in Molecules Viewpoint. *J. Phys. Chem.* **1994**, *98*, 4591–4593.
- (61) Poon, T.; Mundy, B. P.; Shattuck, T. W. The Michael Reaction. *J. Chem. Educ.* **2002**, *79*, 264–267.
- (62) March, J. *Advanced Organic Chemistry, Reactions, Mechanisms, and Structure*; Wiley-Interscience: New York, 1992.
- (63) Joseph-Nathan, P.; Mendoza, V.; Garcia, E. Structure and Proton Magnetic Resonance Study of 3-(N'-Aziridinyl)succinimides. *J. Org. Chem.* **1972**, *37*, 3950–3952.
- (64) Mustafa, A.; Asker, W.; Khattab, S.; Zayed, S. M. A. D. On the Reactivity of the Unsaturated System in TV-Arylmaleimides. *J. Org. Chem.* **1961**, *26*, 787–789.
- (65) Joseph-Nathan, P.; Mendoza, V.; G, E. G. Aziridine Induced Isomerization of Isomaleimides to Maleimides. *Can. J. Chem.* **1974**, *52*, 129–131.
- (66) Ashton, P. R.; Calcagno, P.; Spencer, N.; Harris, K. D. M.; Philp, D. Using Polarization Effects to Alter Chemical Reactivity: A Simple Host Which Enhances Amine Nucleophilicity. *Org. Lett.* **2000**, *2*, 1365–1368.
- (67) Bi, Y.; Bailly, L.; Marsais, F.; Levacher, V.; Papamicaël, C.; Dupas, G. Chemoselective, accelerated and stereoselective aza-Michael addition of amines to N-phenylmaleimide by using TMEDA based receptors. *Tetrahedron: Asymmetry* **2004**, *15*, 3703–3706.
- (68) Hartlen, K. D.; Ismaili, H.; Zhu, J.; Workentin, M. S. Michael Addition Reactions for the Modification of Gold Nanoparticles Facilitated by Hyperbaric Conditions. *Langmuir* **2012**, *28*, 864–871.
- (69) Uno, B. E.; Dicken, R. D.; Redfern, L. R.; Stern, C. M.; Krzywicki, G. G.; Scheidt, K. A. Calcium(II)-catalyzed enantioselective conjugate additions of amines. *Chem. Sci.* **2018**, *9*, 1634–1639.
- (70) Uno, B. E.; Deibler, K. K.; Villa, C.; Raghuraman, A.; Scheidt, K. A. Conjugate Additions of Amines to Maleimides via Cooperative Catalysis. *Adv. Synth. Catal.* **2018**, *360*, 1719–1725.
- (71) Ruesgas-Ramón, M.; Figueroa-Espinoza, M. C.; Durand, E. Application of Deep Eutectic Solvents (DES) for Phenolic Compounds Extraction: Overview, Challenges, and Opportunities. *J. Agric. Food Chem.* **2017**, *65*, 3591–3601.
- (72) Zhao, Y.; Truhlar, D. G. Density Functionals with Broad Applicability in Chemistry. *Acc. Chem. Res.* **2008**, *41*, 157–167.
- (73) Frisch, M. J.; Trucks, G. W.; Schlegel, H. B.; Scuseria, G. E.; Robb, M. A.; Cheeseman, J. R.; Scalmani, G.; Barone, V.; Mennucci, B.; Petersson, G. A.; et al. *Gaussian 09*; Gaussian, Inc.: Wallingford, CT, USA, 2009.
- (74) Grimme, S. Density functional theory with London dispersion corrections. *Wiley Interdiscip. Rev. Comput. Mol. Sci.* **2011**, *1*, 211–228.
- (75) Steinmann, S. N.; Piemontesi, C.; Delachat, A.; Corminboeuf, C. Why are the Interaction Energies of Charge-Transfer Complexes Challenging for DFT? *J. Chem. Theory Comput.* **2012**, *8*, 1629–1640.
- (76) Chandrasekhar, J.; Smith, S. F.; Jorgensen, W. L. Theoretical examination of the SN<sub>2</sub> reaction involving chloride ion and methyl chloride in the gas phase and aqueous solution. *J. Am. Chem. Soc.* **1985**, *107*, 154–163.
- (77) van Megen, W.; Schöpe, H. J. The cage effect in systems of hard spheres. *J. Chem. Phys.* **2017**, *146*, 104503.
- (78) Bryant, S. J.; Atkin, R.; Warr, G. G. Spontaneous vesicle formation in a deep eutectic solvent. *Soft Matter* **2016**, *12*, 1645–1648.
- (79) Fukui, K. Formulation of the reaction coordinate. *J. Phys. Chem.* **1970**, *74*, 4161–4163.
- (80) Gonzalez, C.; Schlegel, H. B. An improved algorithm for reaction path following. *J. Chem. Phys.* **1989**, *90*, 2154–2161.
- (81) Laidler, K. J. *Chemical Kinetics*; Harper Collins Publishers: New York, 1987; pp 112–115.
- (82) Aranda, C.; Richaud, A.; Méndez, F.; Domínguez, A. Theoretical rate constant of methane oxidation from the conventional transition-state theory. *J. Mol. Model.* **2018**, *24*, 294.